JOURNAL OF COMPUTATIONAL PHYSICS 56, 93–110 (1984)

Spectral Estimation through Cubic-Spline Approximation of a Discrete Time Series

NOBUHIRO MORISHIMA

Department of Nuclear Engineering, Kyoto University, Sakyo-ku, Kyoto 606, Japan

Received March 29, 1983; revised February 7, 1984

A method for obtaining accurately the Fourier transform of continuous data is developed. A discrete time series is generated by uniformly sampling the data during a finite period. The method is based on cubic-spline approximation of the data. An analytical expression for the Fourier coefficients is derived in explicit form. The fast Fourier transform (FFT) algorithm is used in the numerical computations. A new procedure to estimate spectrum and correlation functions for continuous random data is developed. The intrinsic properties of the procedure are clarified through a series of test computations.

1. INTRODUCTION

Spectral analysis of random data reveals statistical properties of dynamical systems in many fields of science and engineering. Most of the methods used for performing Fourier transform are based on the fast Fourier transform (FFT) technique for a discrete time series [1]. With the aid of the FFT, both spectrum and correlation functions are rapidly computed. The numerical integration rule of the FFT is equivalent to the trapezoidal rule with additional properties [2], and, hence, gives very crude results for finite Fourier integrals. A simple method for improving accuracy in the use of the FFT is presented by Abramovici [3], who proposes a trapezoidal FFT which does not require a time series to be periodic over an integration interval. Removal of a linear trend improves the accuracy of the FFT results.

Accordingly, for better accuracy, a higher-order numerical quadrature formula is used, though computational speed is sacrificed in some degree. The classical quadrature for this type of integral is Filon's method [4] which reduces to Simpson's rule when a frequency is equal to zero. An extension of Filon's method is found in [5], in [6] where fifth-degree polynomials are used, and in [7] where speed and accuracy are achieved by associating the FFT with Filon's method. Results using Filon's method are accurate only for small values of frequency or for a reasonably smooth integrand. This restriction is due largely to the fact that the derivative of the parabola approximation is discontinuous at every two sampling points. A promising approach is to obtain a continuous approximate function passing through all data

0021-9991/84 $3.00

points smoothly. Ostrander [8] proposes the use of a spline-function approximation in finite Fourier transform and shows how even a linear-spline interpolation reduces errors introduced by the discrete Fourier transform. Numerical evaluation of Fourier integrals with help of B-spline is presented by Lax and Agrawal [11]. Their method is particularly useful as a Fourier transform when the input function, whose Fourier integral is desired, has jumps in value, in slope, or in higher derivatives. Several applications of the method show that proper nonuniform spacing of knots, which optimizes a B-spline fit to the function, produces highly accurate results.

The purpose of the present paper is twofold, i.e., (1) to develop an efficient numerical method for obtaining accurate results of finite Fourier transform from a discrete time series $\{x_n\}$, and (2) to apply this method to the estimation of spectrum and correlation functions for continuous data of time having sample values $\{x_n\}$. The method, to be referred to as the spline-function method (SFM), is based on replacing $\{x_n\}$ with a smooth interpolation curve using a natural cubic-spline function. An advantage of spline interpolation is that a criterion of smoothness is apparent in the sense of the minimum curvature property, and that strong convergence of the spline approximation to an approximated function as a sampling interval approaches zero has been also proved [9]. The finite Fourier transform of the spline-function approximation is performed analytically and obtained in an explicit form. The expression of complex Fourier series allows the use of the FFT in numerical computations. A significant improvement in numerical accuracy is also achieved by use of a few extra points at the boundaries of the integration interval, in order to diminish the influence of the condition on the end derivatives [10]. On the basis of the spline-function method, a new procedure for the spectral estimation is then developed. A series of quantitative tests on spectrum and correlation functions clarifies the intrinsic properties of the procedure and the spline-function method, such as, for example, the accurate estimation property especially to a slowly-varying signal, the strong convergence property with an increase in the sampling rate, and the low sensitivity to round-off errors.

2. Spline-Function Method of Fourier Transform

The discrete time series taken here is samples of data generated from a continuous signal $x(t)$ of time t with an equidistant sampling interval h, and denoted as $\{x_n\}$ where the integer n is the time index, i.e., $t = nh$ for $n = 0, 1, 2, \ldots, N$. To approximate $x(t)$, a cubic-spline function is used, which interpolates all the values $\{x_n\}$ smoothly in the sense of both minimum curvature and numerical stability due to round-off errors. The required expression $S(t)$ for the cubic-splines can be obtained by the following conditions [9]:

(a) The function $S(t)$ is a picewise polynomial of degree 3 such that

$$S(t) = a_n(t - nh)^3 + b_n(t - nh)^2 + c_n(t - nh) + d_n \tag{1}$$

in each interval $nh \leqslant t \leqslant (n + 1)h$ for $n = 0, 1, 2, \ldots, N - 1$.

(b) The function $S(t)$ passes through the values $\{x_n\}$ so that

$$S(nh) = x_n, \qquad \text{i.e., } d_n = x_n \text{ for } n = 0, 1, 2, \ldots, N. \tag{2}$$

(c) The first and second derivatives are continuous at $t = nh$ for $n = 1, 2, \ldots, N-1$, which condition yields

$$a_n = (M_{n+1} - M_n)/6h, \tag{3}$$

$$b_n = M_n/2, \tag{4}$$

$$c_n = -M_n h/3 - M_{n+1} h/6 + (x_{n+1} - x_n)/h, \tag{5}$$

where M_n is the second derivative at $t = nh$ such that

$$M_0 = M_N = 0 \qquad \text{as natural cubic-spline,} \tag{6}$$

$$M_n = 3h^{-2} \sum_{i=0}^{N} (A_{n,i-1} - 2A_{n,i} + A_{n,i+1}) x_i \qquad \text{for} \quad n = 1, 2, \ldots, N-1, \tag{7}$$

with

$$A_{n,-1} = A_{n,0} = A_{n,N} = A_{n,N+1} = 0, \tag{8}$$

$$A_{n,i} = \begin{cases} \dfrac{(-1)^{i-n}}{\sqrt{3}(2+\sqrt{3})^{i-n}} \dfrac{(1-\varepsilon^n)(1-\varepsilon^{N-i})}{1-\varepsilon^N} & \text{for} \quad 1 \leqslant n \leqslant i \leqslant N-1, \\ \dfrac{(-1)^{n-i}}{\sqrt{3}(2+\sqrt{3})^{n-i}} \dfrac{(1-\varepsilon^i)(1-\varepsilon^{N-n})}{1-\varepsilon^N} & \text{for} \quad 1 \leqslant i \leqslant n \leqslant N-1, \end{cases} \tag{9}$$

$$\varepsilon = 7 - 4\sqrt{3} \ (0 < \varepsilon \ll 1). \tag{10}$$

Note that the second derivatives (6) at the end points are introduced to obtain the best cubic-splines of interpolation in the sense of the minimum curvature property. In some cases, however, such a specific condition on the end-derivatives influences the numerical accuracy of the Fourier integrals: a few examples will be given later. To diminish this influence, a few extra points at the boundaries are used. Then the time series $\{x_n\}$ of length $N+1$ is composed of N_e extra points at each boundary and of $N_f + 1$ points used for the Fourier transform, that is,

$$N + 1 = 2N_e + (N_f + 1). \tag{11}$$

Figure 1 illustrates the composition of the time series $\{x_n\}$.

Then the Fourier transform of the sline fit $S(t)$ is defined by the formula

$$F(f) = T^{-1} \int_{N_e h}^{N_e h + T} S(t)\, e^{-i2\pi ft}\, dt, \tag{12}$$

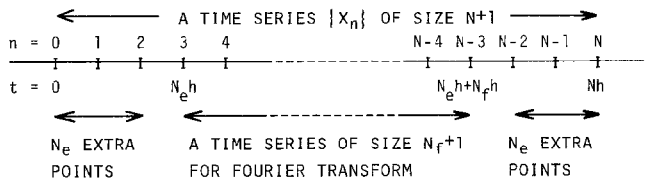

FIG. 1. Composition of the time series $\{x_n\}$ of length $N+1$ for use in Fourier transform. An example of $N_e = 3$ is shown.

where T is the integration interval given by $T = N_f h$. The Fourier integral is rewritten as

$$F(f) = T^{-1} \sum_{n=N_e}^{N_e+N_f-1} \int_{nh}^{(n+1)h} S(t)\, e^{-i2\pi ft}\, dt. \tag{13}$$

Substituting $S(t)$ of Eq. (1) in Eq. (13) and integrating with respect to t, the explicit Fourier coefficients become

$$\begin{aligned} F(f) = {} & N_f^{-1} g_3(f) \sum_{n=N_e}^{N_e+N_f-1} a_n\, e^{-i2\pi fhn} + N_f^{-1} g_2(f) \sum_{n=N_e}^{N_e+N_f-1} b_n e^{-i2\pi fhn} \\ & + N_f^{-1} g_1(f) \sum_{n=N_e}^{N_e+N_f-1} c_n\, e^{-i2\pi fhn} + N_f^{-1} g_0(f) \sum_{n=N_e}^{N_e+N_f-1} d_n e^{-i2\pi fhn}, \end{aligned} \tag{14}$$

where $g_j(f)$ for $j = 0, 1, 2$, and 3 is an analytic function of frequency f, and readily obtained by evaluating the itegral

$$g_j(f) = \int_0^1 t^j e^{-i2\pi fht}\, dt. \tag{15}$$

Formula (14) numerically computes Fourier coefficients of complex value. There are two main ways of doing this: (1) Compute directly the right-hand side of Eq. (14) for arbitrarily selected values of frequency f and sample size N_f. This entire calculation, however, is likely to require lengthy computation times due to the four kinds of summation, especially when made for various frequencies and large sample size. (2) Introduce the FFT algorithm for computing the summations in formula (14). This calculation is limited to the case where the size N_f is equal to an integer power of 2. Nevertheless, a significant reduction in computation time is achieved. Furthermore, a set of Fourier coefficients for such frequencies that

$$f = k/T \qquad \text{for} \quad k = 0, 1, 2, \ldots, N_f/2, \tag{16}$$

where the upper frequency limit is $1/2h$, i.e., the Nyquist frequency, is easily obtained.

The finite series of Fourier coefficients thus obtained is insufficient to reproduce $x(t)$, because it is represented by an infinite Fourier series as

$$x(t) = \sum_{k=-\infty}^{+\infty} F(k/T)\, e^{-i2\pi kt/T}, \qquad N_e h \leqslant t \leqslant N_e h + T. \tag{17}$$

In practice, the number of required Fourier coefficients will be limited, and, in some cases, may be the same degree with $N_f/2$. In this case, formula (17) with summation for k from $-N_f/2$ to $N_f/2$ is used in order to assess the approximation to $x(t)$ at discrete time $t = nh$ for $n = N_e$, $N_e + 1$, $N_e + 2$,..., $N_e + N_f$. This assessment can be easily performed by use of an FFT algorithm.

3. Procedure for Spectral Estimation

The spline-function method of Fourier transform produces a new procedure for estimating spectrum and correlation functions for the continuous-time signal $x(t)$. The main steps of the procedure are summarized in the flow graph in Fig. 2. An ordinary procedure applicable to discrete time series $\{x_n\}$ is also shown for reference. Pre- and

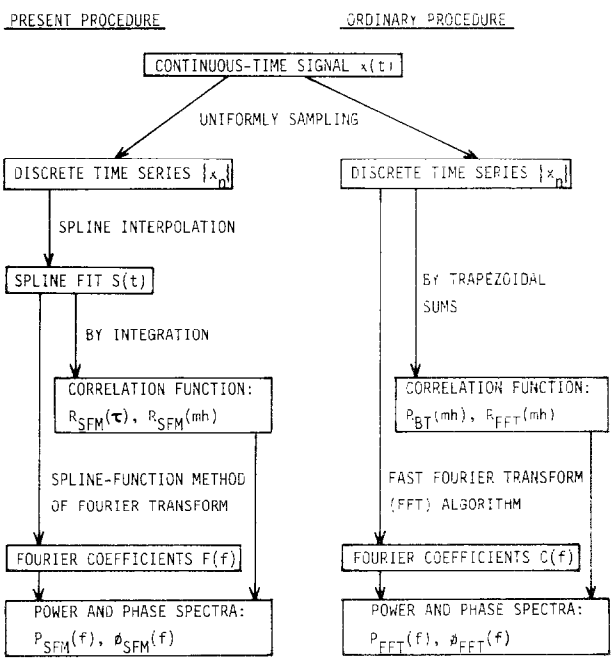

FIG. 2. A graphic representation of the present procedure for estimating the spectral and correlation functions for the noise signal $x(t)$. Also shown is an ordinary procedure used for the discrete time series $\{x_n\}$.

post-processing modes such as trend removal and time- or spectral-window operation are excluded. The following development is confined to an analysis of one-dimensional process represented by $\{x_n\}$.

The set of the Fourier coefficients $F(f)$ calculated numerically using the spline-function method is used to obtain the power spectrum $P_{\mathrm{SFM}}(f)$ and the phase spectrum $\phi_{\mathrm{SFM}}(f)$, namely,

$$P_{\mathrm{SFM}}(f) = T|F(f)|^2 \qquad (1/\mathrm{Hz}), \tag{18}$$

$$\phi_{\mathrm{SFM}}(f) = \arctan(\mathrm{Im}[F(f)]/\mathrm{Re}[F(f)]). \tag{19}$$

The correlation function for continuous lag time τ is defined in terms of the spline fit $S(t)$ for the period from $N_e h$ to $(N_e + N_f)h$ (see Fig. 1), such that

$$R_{\mathrm{SFM}}(\tau) = (T-\tau)^{-1} \int_{N_e h}^{N_e h + T - \tau} S(t+\tau)\, S(t)\, dt, \qquad 0 \leqslant \tau \leqslant T. \tag{20}$$

The integral in Eq. (20) is solved analytically by substituting $S(t)$ of Eq. (1) in the integrand and integrating with respect to t. Detailed procedures for the integration are described in Appendix A. An explicit expression of $R_{\mathrm{SFM}}(\tau)$ is given by Eq. (A.8). In particular, in the case of discrete values of τ such as $\tau = mh$ for $m = 0$ or integer, the correlation function becomes considerably simpler:

$$\begin{aligned} R_{\mathrm{SFM}}(mh) = (N_f - m)^{-1} \sum_{n=0}^{N_f - m - 1} & [a_i a_j h^6/7 + (a_i b_j + b_i a_j)\, h^5/6 \\ & + (a_i c_j + b_i b_j + c_i a_j)\, h^4/5 \\ & + (a_i d_j + b_i c_j + c_i b_j + d_i a_j)\, h^3/4 + (b_i d_j + c_i c_j + d_i b_j)\, h^2/3 \\ & + (c_i d_j + d_i c_j)\, h/2 + d_i d_j], \end{aligned} \tag{21}$$

where

$$i = N_e + n + m \qquad \text{and} \qquad j = N_e + n.$$

Two comments on the results (18) through (21) follow. (1) The continuous correlation function (A.8) is used to determine the corresponding spectral density. It is necessary to begin with uniformly sampling the function (A.8) at equidistant time intervals to obtain a time series as discrete representation of the function (A.8). The Fourier transform of the time series is determined using the spline-function method, and gives the desired spectral estimate. (2) The significance of the results (18) through (21) is easily understood by showing how these results are reduced to the corresponding ones used in ordinary procedures for spectral estimation. Provided that splines of degree zero are applied to the interpolation of the time series $\{x_n\}$, the result in the nth interval is

$$S(t) = x_n. \tag{22}$$

This corresponds to Eq. (1) with $a_n = b_n = c_n = 0$ and is equivalent to using a trapezoidal rule in interpolation. Thus the familiar expression for Fourier coefficients is

$$C(f) = N_f^{-1} \sum_{n=N_e}^{N_e+N_f-1} x_n e^{-i2\pi fhn}. \tag{23}$$

The power spectrum $P_{FFT}(f)$ and the phase spectrum $\phi_{FFT}(f)$ which arise in an FFT procedure are rapidly computed by use of the FFT in the calculation of Eq. (23). The correlation function (21) reduces to the form associated with a Blackman–Tukey procedure, as shown by

$$R_{BT}(mh) = (N_f - m)^{-1} \sum_{n=0}^{N_f-m-1} x_{N_e+n+m} x_{N_e+n}. \tag{24}$$

Allowing cyclic use of $\{x_n\}$ such as $x_{N_e+n} = x_{N_e+N_f+n}$ produces another expression $R_{FFT}(mh)$ for correlation function as is usual with an FFT procedure.

4. Intrinsic Properties of the Spline-Function Method

The spline-function method has been applied to a set of artificial time series generated from uniform sampling of various deterministic functions. The functions and sampling conditions are listed in Table I. All the time series are classified conveniently into five major groups; hereafter they will be represented by the symbol $\{x_n\}_l$ ($l = 1, 2, 3, 4, 5$). The sample size N_f is always taken to be equal to an integer power of 2, since the FFT algorithm can be fully utilized in calculating Eq. (14). The computations were done on a FACOM-382 in single precision, about seven significant decimal digits.

4.1. *Intrinsic Properties on Power and Phase Spectra*

The spectra $P_{SFM}(f)$ and $\phi_{SFM}(f)$ have been compared with the exact results $P_E(f)$ and $\phi_E(f)$ which are calculated directly from the functions listed in Table I. The comparison is made in terms of the relative deviations of $P_{SFM}(f)$ and $\phi_{SFM}(f)$ from the exact ones, i.e.,

$$D^P_{SFM}(f) = |[P_{SFM}(f) - P_E(f)]/P_E(f)| \times 100\ (\%), \tag{25}$$

$$D^\phi_{SFM}(f) = |[\phi_{SFM}(f) - \phi_E(f)]/\phi_E(f)| \times 100\ (\%). \tag{26}$$

For reference, another comparison is given of $P_{FFT}(f)$ and $\phi_{FFT}(f)$ with the exact ones, such that

$$D^P_{FFT}(f) = |[P_{FFT}(f) - P_E(f)]/P_E(f)| \times 100\ (\%), \tag{27}$$

$$D^\phi_{FFT}(f) = |[\phi_{FFT}(f) - \phi_E(f)]/\phi_E(f)| \times 100\ (\%). \tag{28}$$

TABLE I

Test Functions and Sampling Conditions for Producing Artificial Time Series

$\{x_n\}_l$	Test functions of time t	Sampling conditions		
		h (s)	$N+1$ (N_e, N_f)[a]	α (s^{-1}), f_0 (Hz), and θ (rad)
$\{x_n\}_1$	$e^{-\alpha t}$	0.1	65(0, 64) 71(3, 64) 75(5, 64)	$\alpha = 0.25, 0.5, 1, 2, 5$
$\{x_n\}_2$	$\cos(2\pi f_0 t + \theta)$	0.1	65(0, 64) 71(3, 64)	$f_0 = 0.9375$, $\theta = -2\pi f_0 N_e h + 0.125\pi l$ for integer l from 0 to 16
$\{x_n\}_3$	$\cos(2\pi f_0 t + \theta)$	0.1	71(3, 64)	$f_0 = 0.15625l$ for $l = 6, 7, 8, 9, 11, 13, 16, 21, 32$ $\theta = -2\pi f_0 h N_e + 0.25\pi$
$\{x_n\}_4$	$e^{-\alpha t}\cos(2\pi f_0 t + \theta)$	0.2 0.1 0.05 0.025	39(3, 32) 71(3, 64) 135(3, 128) 263(3, 256)	$\alpha = 2.0$ $f_0 = 0.9375$ $\theta = -2\pi f_0 h N_e + 0.25\pi$
$\{x_n\}_5$	$e^{-\alpha t}\cos(2\pi f_0 t + \theta)$	0.1	71(3, 64)	$\alpha = 2.0$, $f_0 = 0.15625 \times 2^l$ for $l = -\infty, -5, -4, \ldots, 3, 4$ $\theta = -2\pi f_0 h N_e$

[a] The mutual relation of N, N_e, and N_f is given by Eq. (11) and shown in Fig. 1.

The computation time in calculating the spline fit is minimized by computing $A_{n,i}$ only for values of $|n-i|$ not exceeding integer j, thus taking $A_{n,i} = 0$ for $|n-i| > j$. The value of j is decided in terms of the convergence of $P_{SFM}(f)$ and $\phi_{SFM}(f)$ calculated from the time series $\{x_n\}_4$ with individual values of j varying from zero up to 10. Figure 3 shows the two kinds of ratios with respect to $P_{SFM}(f)$ and $\phi_{SFM}(f)$: the ratios of the relative deviation $D^P_{SFM}(f)$ computed for each j to that for $j = 10$ and the ratios of $D^\phi_{SFM}(f)$ for each j to that for $j = 10$. The results of these calculations enable us to decide to take $j = 8$, which is adopted in the following analysis.

(1) *Influence of the end condition* (6). The influence of the end condition (6) on spectral estimates is studied by varying the size of extra points N_e but keeping the sample size N_f constant (see Fig. 1). Figures 4 and 5 illustrate $D^P_{SFM}(f)$ and $D^\phi_{SFM}(f)$, respectively, obtained from $\{x_n\}_1$ for $N_e = 0$, 3, and 5. Also shown are $D^P_{FFT}(f)$ and $D^\phi_{FFT}(f)$ for reference. The introduction of only three extra points is found to improve the numerical accuracy remarkably. For the smaller values of α, no distinct deviations in spectral estimates are observed. The effectiveness of a few extra points is demonstrated by spectral analysis of $\{x_n\}_2$ which obtains spectral estimates of $x(t) = \cos(2\pi f_0 t + \theta)$ by systematically varying the initial phase θ. Figure 6 illustrates

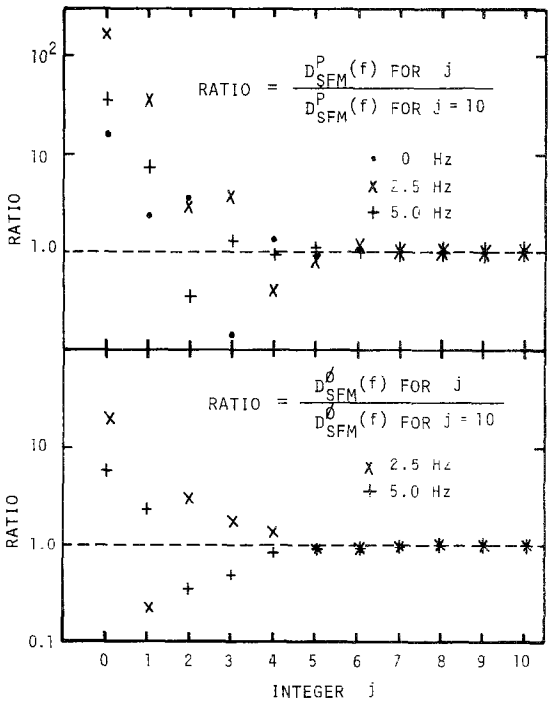

FIG. 3. The convergence of the spectra $P_{SFM}(f)$ and $\phi_{SFM}(f)$ with an increase in j.

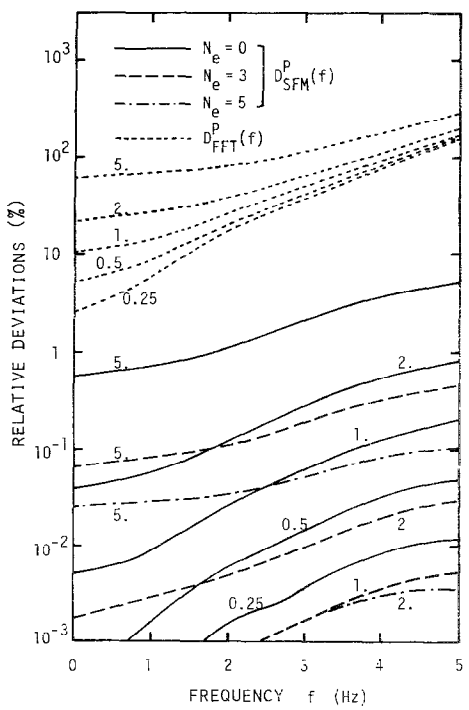

FIG. 4. The influence of the end condition (6) on power spectrum. Shown are the relative deviations $D^P_{SFM}(f)$ for $N_e = 0$, 3, and 5, together with $D^P_{FFT}(f)$. The numerals shown correspond to those of α of $\{x_n\}_1$ in Table I.

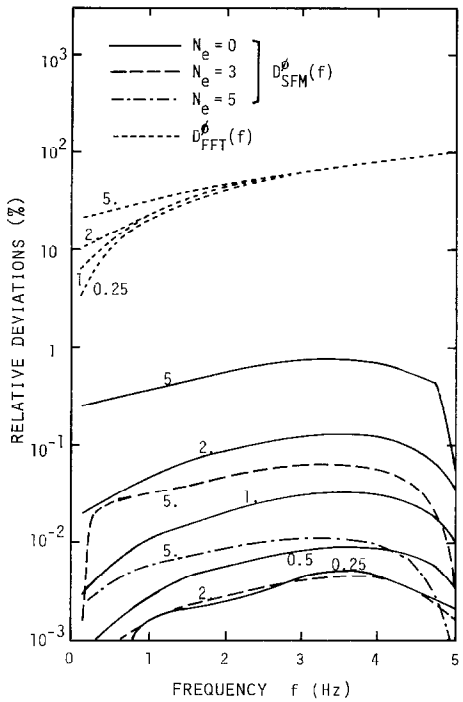

FIG. 5. The influence of the end condition (6) on phase spectrum. Shown are the relative deviations $D^{\phi}_{SFM}(f)$ for $N_e = 0, 3$, and 5, together with $D^{\phi}_{FFT}(f)$. The numerals shown correspond to those of α of $\{x_n\}_1$ in Table I.

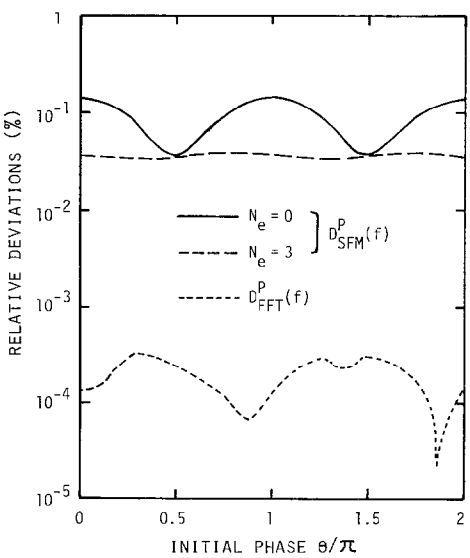

FIG. 6. The influence of the end condition (6) on the peak of power spectrum at frequency of $f_0 = 0.9375$ Hz. Shown are the relative deviations $D^{P}_{SFM}(f_0)$ for $N_e = 0$ and 3, together with $D^{P}_{FFT}(f_0)$.

$D^P_{SFM}(f_0)$ at a frequency of $f_0 = 0.9375$ Hz for $N_e = 0$ and 3, together with $D^P_{FFT}(f_0)$. It is clear that using three extra points results in uniformly accurate power spectrum for all values of θ. Also, for $N_e = 0$, $D^P_{SFM}(f_0)$ becomes maximum when θ is equal to zero (i.e., $x(0) = 1$) or to π (i.e., $x(0) = -1$). This is due to the deviation of the spline fit $S(t)$ from the original function $x(t)$ at the end points, which strongly affects the finite Fourier integral (12).

(2) *Estimation property to the periodic signal.* As shown in Figs. 4 and 5, the spline-function method produces spectral estimates with small relative deviations not exceeding 0.5% in the case of $N_e = 3$, while the FFT gives rise to a large relative deviation. Figure 6 shows that the FFT method produces almost exact answers, while the spline-function method indicates constant relative deviations of about 0.035%. These results imply as follows: (a) The spline-function method is suitable for use in a slowly varying time series relative to a sampling interval h such as, for example, $\{x_n\}_1$ and $\{x_n\}_4$: the analysis of the latter will be presented later. (b) The FFT is good to estimate the frequency with which the signal $x(t)$ varies periodically.

The above properties of both methods have been checked for a peak of the spectral estimates calculated from $\{x_n\}_3$. The relative deviations are obtained for various values of the frequency f_0 where the initial phase of the test function maintains a constant value of 0.25π. The resultant relative deviations are plotted in Fig. 7 against

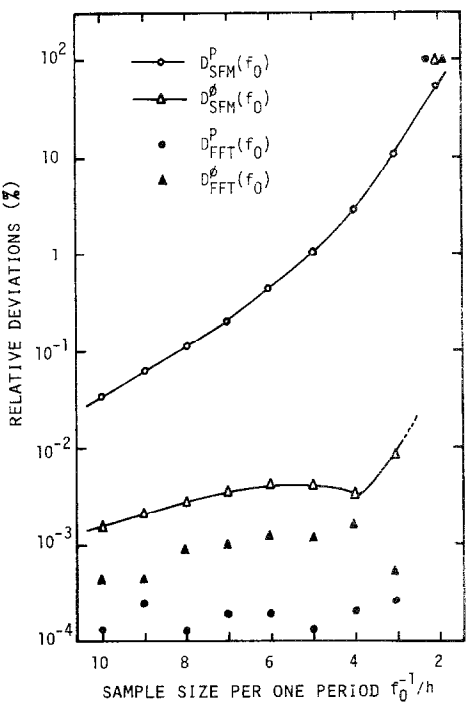

FIG. 7. The relative deviations of spectral estimates from the exact ones for various values of the frequency f_0 listed in Table I under the item of $\{x_n\}_3$.

the number of sampling per one period, i.e., f_0^{-1}/h. The results $D^P_{\mathrm{SFM}}(f_0)$ are observed to approach $D^P_{\mathrm{FFT}}(f_0)$ with an increase in f_0^{-1}/h, thus indicating the above-mentioned properties. It can also be seen that the accuracy of the phase spectra is about the same for both methods.

(3) *Convergence property.* The convergence of spectral estimates to the exact ones depends ultimately on the smoothness of the original signal $x(t)$ which is relative to the sampling conditions such as the interval h and the size N_f. An example of this has been given in Fig. 7 with respect to fast convergence by varying the frequency f_0 of the periodic signal, but keeping N_f constant. Another example is chosen to illustrate how the spline-function method improves in accuracy as h decreases under the condition of keeping hN_f constant. The next spectral analysis is given of $\{x_n\}_4$. The results of the analysis are shown in Figs. 8 and 9 in terms of the relative deviations of power and phase spectra, respectively. It is readily seen that the spline-function method has a good property of convergence for both spectral estimates over the wide frequency range from zero to the Nyquist frequency. The results of the cases 3 and 4 for frequency above 5 Hz are not presented. Distinct difference in rate of

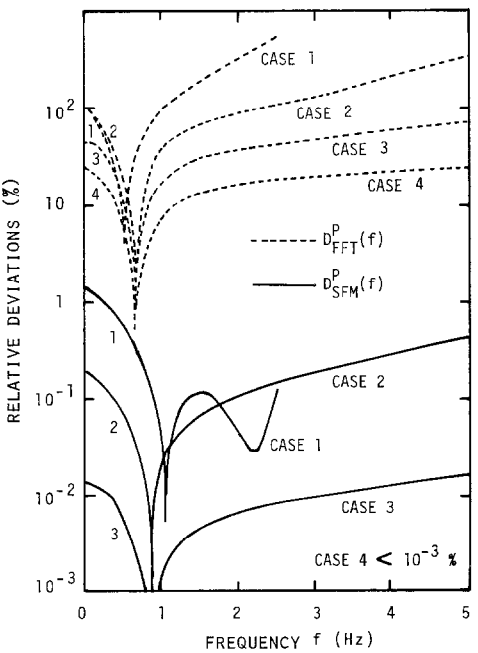

FIG. 8. The convergence property of the power spectra with an increase in sampling rate $1/h$ under the condition of hN_f = constant. Shown are the relative deviations $D^P_{\mathrm{SFM}}(f)$ and $D^P_{\mathrm{FFT}}(f)$ for the four different cases: case 1 of $h = 0.2$ s and $N_f = 32$, case 2 of $h = 0.1$ s and $N_f = 64$, case 3 of $h = 0.05$ s and $N_f = 128$, and case 4 of $h = 0.025$ s and $N_f = 256$.

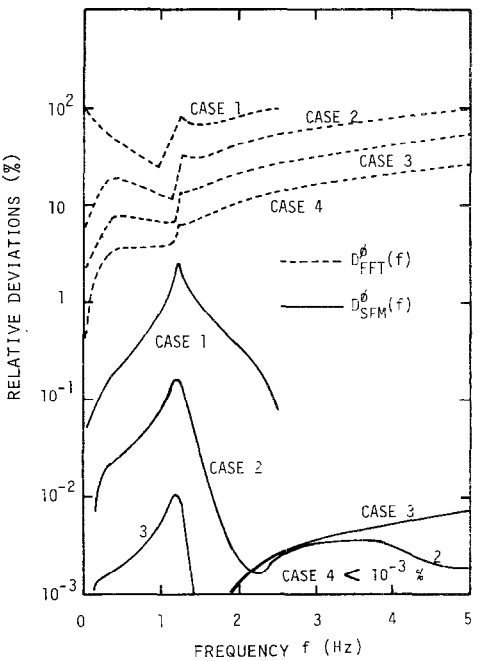

FIG. 9. The convergence property of the phase spectra with an increase in sampling rate $1/h$ under the condition of $hN_f = \text{constant}$. Shown are the relative deviations $D^{\phi}_{\text{SFM}}(f)$ and $D^{\phi}_{\text{FFT}}(f)$ for the same cases as described in Fig. 8.

convergence between the two methods is observed, due mainly to the excellent interpolation property of the spline-function method in comparison with the FFT based on trigonometric approximation of a time series $\{x_n\}$.

4.2. *Intrinsic Properties on Correlation Function*

As time-domain assessment of the present procedure, a correlation analysis has been performed of $\{x_n\}_5$. A typical example of the analysis is presented in Fig. 10 for $f_0 = 0.0391$ Hz, which illustrates the exact correlation function $R_{\text{E}}(\tau)$ calculated using the definition (20), and the relative deviations from $R_{\text{E}}(\tau)$ such that

$$D^R_X(mh) = |[R_X(mh) - R_{\text{E}}(mh)]/R_{\text{E}}(mh)| \times 100\ (\%), \tag{29}$$

where X is the subscript indicating the present procedure by SFM, the Blackman–Tukey procedure by BT, and the FFT procedure by FFT. The results $D^R_{\text{SFM}}(mh)$ show negligible relative deviations. Most of $D^R_{\text{SFM}}(mh)$ for other values of f_0 are also found to be much the same, though they are not presented here. It is convenient to express $D^R_{\text{SFM}}(mh)$ as well as $D^R_{\text{BT}}(mh)$ and $D^R_{\text{FFT}}(mh)$ in terms of the average D^R_X and the standard deviation δD^R_X from D^R_X, given by

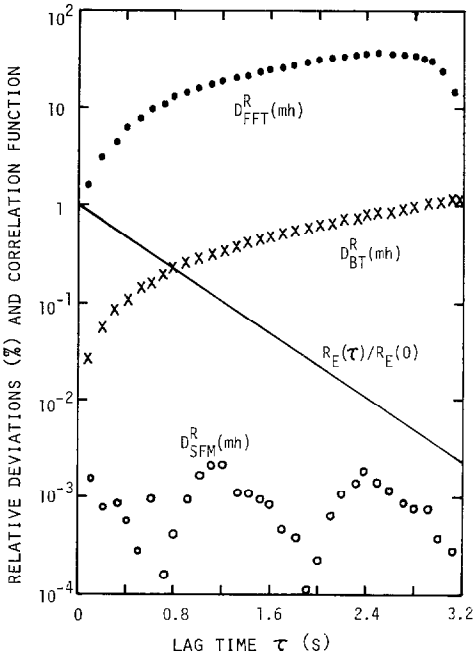

FIG. 10. A typical example of the correlation-function analysis of $\{x_n\}_5$ for $f_0 = 0.0391$ Hz. Shown are the normalized exact correlation function $R_E(\tau)/R_E(0)$ and the relative deviations $D_X^R(mh)$ for $X = \text{SFM, BT, and FFT}$.

$$D_X^R = M^{-1} \sum_{m=0}^{M} D_X^R(mh), \tag{30}$$

$$\delta D_X^R = \left[M^{-1} \sum_{m=0}^{M} (D_X^R(mh) - D_X^R)^2 \right]^{1/2}, \tag{31}$$

where the maximum lag M is taken to be equal to one-half the sample size, i.e., $M = 32$.

Figure 11 shows each of D_X^R and $D_X^R + \delta D_X^R$ against the set of values of the frequency f_0 ranging from zero up to one-half the Nyquist frequency. The present procedure gives the best approximation to the required answer $R_E(\tau)$ within an average relative deviation of less than 0.03%, except for the case of $f_0 = 2.5$ Hz. The Blackman–Tukey procedure produces considerable deviations especially for the larger values of f_0. This is due to the trapezoidal approximation of the integral (20). The large deviations of the FFT procedure are due to two major causes: In the region of $f_0 \gtrsim 0.08$ Hz, i.e., smaller sampling rate per one period f_0^{-1}, it is attributed to much the same with the results of the Blackman–Tukey procedure. In the other region, it is caused by whether or not the circular correlation function is used.

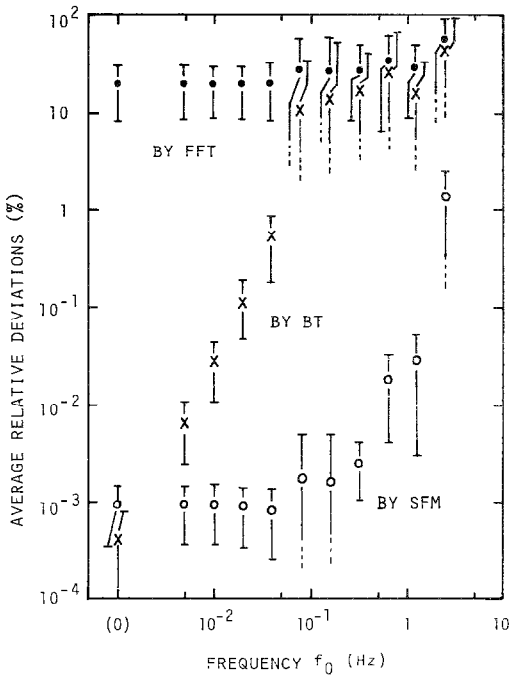

FIG. 11. The variations in the relative deviations of the correlation functions $R_X(mh)$ from $R_E(mh)$ for the various values of the frequency f_0 listed in Table I under the item of $\{x_n\}_5$. Shown are the average relative deviations D_X^R and the error bars $D_X^R \pm \delta D_X^R$ for the present procedure ($X = \text{SFM}$), the Blackman–Tukey procedure ($X = \text{BT}$), and the FFT procedure ($X = \text{FFT}$).

5. CONCLUDING REMARKS

(a) A new method has been developed for estimating the finite Fourier transform of a continuous-time signal $x(t)$ based on a cubic-spline interpolation to $\{x_n\}$ and an analytic integration of the spline functions. The method does not require $x(t)$ to be periodic over an integration interval.

(b) To obtain better numerical accuracy of the spectral estimates such as power and phase spectra, the use of a few extra points is effective, thereby diminishing the influence of the extraneously introduced second derivatives at the end points. Another improvement of accuracy occurs with an increase in sampling rate during the fixed period of sampling.

(c) Explicit expressions for the Fourier coefficients $F(f)$ result in a significant reduction in the number of computations, together with a low sensitivity to round-off errors. Use of the FFT algorithm in numerical calculation of $F(f)$ leads to a further reduction in computation time.

(d) The present procedure for spectral analysis is useful for gaining accurate information about original random data $x(t)$. It may be used in assessing the spectral estimates from various approachs to noise-signal processing.

APPENDIX A

The explicit expression for the correlation function $R_{\mathrm{SFM}}(\tau)$ is obtained as follows. A continuous lag time τ may be written in the form

$$\tau = mh + \varepsilon h, \tag{A.1}$$

where m is a maximum integer not exceeding τ/h and $0 \leqslant \varepsilon < 1$. Then the spline fits $S(t+\tau)$ and $S(t)$ in the integrand (20) lie in the integration intervals

$$N_e h + mh + \varepsilon h \leqslant t + \tau \leqslant N_e h + N_f h \qquad \text{and} \qquad N_e h \leqslant t \leqslant N_e h + N_f h - mh - \varepsilon h, \tag{A.2}$$

where $T = N_f h$ is used. Since the spline fit is defined in each interval as in Eq. (1), it requires that the product $S(t+\tau)\,S(t)$ is evaluated in each of the subintervals which are divided into two parts: a series of subintervals of size $(1-\varepsilon)h$ such that

$$(N_e + m + n + \varepsilon)\,h \leqslant t + \tau \leqslant (N_e + m + n + 1)h$$

and (A.3)

$$(N_e + n)h \leqslant t \leqslant (N_e + n + 1 - \varepsilon)h, \qquad \text{for} \quad n = 0, 1, 2, \ldots, N_f - m - 1,$$

and a series of subintervals of size εh such that

$$(N_e + m + n + 1)h \leqslant t + \tau \leqslant (N_e + m + n + 1 + \varepsilon)h$$

and (A.4)

$$(N_e + n + 1 - \varepsilon)h \leqslant t \leqslant (N_e + n + 1)h, \qquad \text{for} \quad n = 0, 1, 2, \ldots, N_f - m - 2.$$

Then the integral in Eq. (20) is rewritten in the form

$$\begin{aligned} R_{\mathrm{SFM}}(\tau) = (T-\tau)^{-1} & \sum_{n=0}^{N_f-m-1} \int_0^{(1-\varepsilon)h} S(N_e h + mh + nh + \varepsilon h + t) \\ & \cdot S(N_e h + nh + t)\,dt \\ & + (T-\tau)^{-1} \sum_{n=0}^{N_f-m-2} \int_0^{\varepsilon h} S(N_e h + mh + nh + h + t) \\ & \cdot S(N_e h + nh + h - \varepsilon h + t)\,dt. \end{aligned} \tag{A.5}$$

Substituting $S(t)$ of Eq. (1) in Eq. (A.5), we have

$$R_{\mathrm{SFM}}(\tau) = (T-\tau)^{-1} \sum_{n=0}^{N_f-m-1} \int_0^{(1-\varepsilon)h} [a_i(\varepsilon h + t)^3 + b_i(\varepsilon h + t)^2 + c_i(\varepsilon h + t) + d_i]$$
$$\cdot [a_j t^3 + b_j t^2 + c_j t + d_j]\, dt$$
$$+ (T-\tau)^{-1} \sum_{n=0}^{N_f-m-2} \int_0^{\varepsilon h} [a_k t^3 + b_k t^2 + c_k t + d_k]$$
$$\cdot [a_j(h - \varepsilon h + t)^3 + b_j(h - \varepsilon h + t)^2 + c_j(h - \varepsilon h + t) + d_j]\, dt, \qquad \text{(A.6)}$$

where

$$i = N_e + m + n, \qquad j = N_e + n, \qquad \text{and} \qquad k = N_e + m + n + 1. \qquad \text{(A.7)}$$

Integrating with respect to t, we get the desired expression

$$R_{\mathrm{SFM}}(\tau) = (N_f - m - \varepsilon)^{-1} \sum_{n=0}^{N_f-m-1} [a_i a_j (1-\varepsilon)^7 h^6/7$$
$$+ (a_i b_j + S_i''(\varepsilon h)\, a_j/2)(1-\varepsilon)^6 h^5/6$$
$$+ (S_i'(\varepsilon h)\, a_j + S_i''(\varepsilon h)\, b_j/2 + a_i c_j)(1-\varepsilon)^5 h^4/5$$
$$+ (S_i(\varepsilon h)\, a_j + S_i'(\varepsilon h)\, b_j + S_i''(\varepsilon h)\, c_j/2 + a_i d_j)(1-\varepsilon)^4 h^3/4$$
$$+ (S_i(\varepsilon h)\, b_j + S_i'(\varepsilon h)\, c_j + S_i''(\varepsilon h)\, d_j/2)(1-\varepsilon)^3 h^2/3$$
$$+ (S_i(\varepsilon h)\, c_j + S_i'(\varepsilon h)\, d_j)(1-\varepsilon)^2 h/2 + S_i(\varepsilon h)\, d_j(1-\varepsilon)]$$
$$+ (N_f - m - \varepsilon)^{-1} \sum_{n=0}^{N_f-m-2} [a_j a_k \varepsilon^7 h^6/7 + (a_j b_k + S_j''(h - \varepsilon h)\, a_k/2)\, \varepsilon^6 h^5/6$$
$$+ (S_j'(h - \varepsilon h)\, a_k + S_j''(h - \varepsilon h)\, b_k/2 + a_j c_k)\, \varepsilon^5 h^4/5$$
$$+ (S_j(h - \varepsilon h)\, a_k + S_j'(h - \varepsilon h)\, b_k + S_j''(h - \varepsilon h)\, c_k/2 + a_j d_k)\, \varepsilon^4 h^3/4$$
$$+ (S_j(h - \varepsilon h)\, b_k + S_j'(h - \varepsilon h)\, c_k + S_j''(h - \varepsilon h)\, d_k/2)\, \varepsilon^3 h^2/3$$
$$+ (S_j(h - \varepsilon h)\, c_k + S_j'(h - \varepsilon h)\, d_k)\, \varepsilon^2 h/2 + S_j(h - \varepsilon h)\, d_k \varepsilon], \qquad \text{(A.8)}$$

where

$$S_l(t) = a_l t^3 + b_l t^2 + c_l t + d_l, \qquad \text{for} \quad l = i \text{ or } j. \qquad \text{(A.9)}$$

For the discrete values of lag time given by $\tau = mh$ where m is zero or integer, the expression (A.8) leads to Eq. (21).

REFERENCES

1. J. S. BENDAT AND A. G. PIERSOL, "Random Data: Analysis and Measurement Procedures," Wiley, New York, 1971.
2. J. W. COOLEY, P. A. W. LEWIS, AND P. D. WELCH, *IEEE Trans. Audio Electroacoust.* **AU-15** (1967), 79.
3. F. ABRAMOVICI, *J. Comput. Phys.* **11** (1973), 28.
4. L. N. G. FILON, *Proc. Roy. Soc. Edingburgh* **49** (1928), 38.
5. P. J. DAVIS AND P. RABINOWITZ, "Methods of Numerical Integration," Academic Press, New York/London, 1975.
6. E. A. FLINN, *J. Assoc. Comput. Mach.* **1** (1960), 181.
7. F. MANDEL AND R. J. BEARMAN, *J. Comput. Phys.* **7** (1971), 637.
8. L. E. OSTRANDER, *IEEE Trans. Audio Electroacoust.* **AU-19** (1971), 103.
9. J. H. AHLBERG, E. N. NILSON, AND J. L. WALSH, "The Theory of Splines and Their Applications," Academic Press, New York/London, 1967.
10. B. EINARSSON, *BIT* **8** (1968), 279.
11. M. LAX AND G. P. AGRAWAL, *Math. Comp.* **39** (1982), 535.